

19th CIRP Conference on Modeling of Machining Operations

Application of material constitutive and friction models parameters identified with AI and ALE to a CEL orthogonal cutting model

François Ducobu^{*,a}, Nithyaraaj Kugalur Palanisamy^a, Pedro-José Arrazola^b, Edouard Rivière-Lorphèvre^a

^aMachine Design and Production Engineering Lab, Research Institute for Science and Material Engineering, University of Mons, 7000 Mons, Belgium

^bMechanical and Manufacturing Department, Faculty of Engineering, Mondragon Unibertsitatea, Loramendi 4, 20500 Arrasate-Mondragón, Spain

* Corresponding author. Tel.: +3265374568. E-mail address: Francois.Ducobu@umons.ac.be

Abstract

The identification of input parameters for finite element modelling of the cutting process is still a complex task as the experimental testing equipment cannot reach its combined levels of strains, strain rates and temperatures. Inverse identification using Artificial Intelligence method provides a relevant alternative. In this paper, material constitutive and friction models parameters identified with an Efficient Global Optimization algorithm and an ALE orthogonal cutting model are introduced in a CEL model. Assessment of the differences in the results due to the formulation and dependence of parameters identification to the finite element model are then performed.

© 2023 The Authors. Published by Elsevier B.V.

This is an open access article under the CC BY-NC-ND license (<https://creativecommons.org/licenses/by-nc-nd/4.0>)

Peer review under the responsibility of the scientific committee of the 19th CIRP Conference on Modeling of Machining Operations

Keywords: Cutting; Finite element method (FEM); Predictive model

1. Introduction

The accuracy of a Finite Element (FE) model for the cutting process is highly dependent on constitutive and friction modelling [1, 2]. This is a difficult task due to the severe conditions in terms of strain, strain rate, temperature, temperature rise, etc. seen by the material during the operation. Identification of the parameters of these models is therefore challenging and the dedicated equipments currently available, such as Split Hopkinson Pressure Bars [3], the Taylor impact test [4], etc., do not allow to reproduce them. The inverse identification method can therefore be an efficient alternative [2]. Using the Levenberg–Marquardt algorithm to identify the constitutive material parameters, Shrot and Bäker [5] highlighted the non-uniqueness of the inverse identification problem: several sets of parameters can lead to similar cutting forces and chip morphology. The rise of Artificial Intelligence (AI) has intensified research in the inverse identification of material parameters, such as in Bosetti et al. [6], Denkena et al. [7] or Bergs et al. [8–10]. Most of the inverse identification works adopt the Johnson-Cook (JC) model as it is the most used in the field, even if it is not the best one,

and has a reasonable number of material constants. To tackle the long computation times, Kugalur Palanisamy et al. [11] introduced an Efficient Global Optimization (EGO) algorithm. They moreover identified the parameters of both material and friction models for the Ti6Al4V titanium alloy. As in previous works, the non-uniqueness of the problem lead to the identification of several sets of parameters.

The software and the formulation used for the development of the FE model have also an influence on the results [12]. Sridhar et al. [13] mainly highlighted the future potential of meshless formulations (by comparison to mesh-based formulations) but with a high computation time. Afrasiabi et al. [14] showed a better prediction of forces with the FE method by comparison to Smoothed Particle Hydrodynamics (SPH). They highlighted that the value of the friction coefficient has more impact on the forces from SPH than from FE. An increasing number of studies focuses on the performance of the recently applied Coupled Eulerian-Lagrangian (CEL) formulation to the simulation of cutting by comparison to more common Lagrangian and Arbitrary Lagrangian-Eulerian (ALE) formulations. According to Ducobu et al. [15], CEL provides a good prediction of chip morphology and cutting forces with a competitive computation time by comparison to ALE. In [16], CEL and ALE results are similar and they are closer to the experimental reference than

Lagrangian with remeshing results. Issues of mesh distortion are not occurring with CEL, while they can prematurely end the computation for the two other formulations. Aridhi et al. [17] obtained similar quantitative results with ALE and CEL formulations, also close to the experimental reference. The reliability of CEL and the absence of dependence of the results to the initial shape of the chip made it the recommended formulation despite its higher computation time. Combining the influence of the formulation (Lagrangian, ALE and CEL) and of the set of JC parameters (two different sets), Zhang et al. [18] showed that the best set of JC parameters is not unique for the three formulations. The authors attributed it to the method adopted by the formulations to simulate material separation.

This paper applies the material and friction models parameters identified for an ALE-Eulerian model [11] to a CEL model [19]. The same software and the same modelling conditions are adopted to allow a rigorous comparison of the results. The aim of this study is therefore to assess the influence of the ALE-Eulerian and CEL formulations and of the set of input parameters (material and friction) on the results of an orthogonal finite element model of Ti6Al4V.

2. Finite Elements models

The orthogonal cutting process is modelled in 2D with ALE-Eulerian and CEL models in plane strain conditions with the software Abaqus/Explicit 2020. The out-of-plane behaviour is not considered as it is assumed to be negligible ($b/h \geq 10$, see Table 1). Cutting conditions are the same and are presented in Table 1. Models characteristics are as close as possible to allow a rigorous comparison. This required a slight modification of the ALE model of Kugalur Palanisamy et al. [11] (see section 2.1).

The workpiece material, Ti6Al4V, is considered as an elastoplastic material with its plastic part described by the well-known Johnson-Cook equation [20]:

$$\sigma = (A + B \varepsilon^n) \left(1 + C \ln \frac{\dot{\varepsilon}}{\dot{\varepsilon}_0} \right) \left(1 - \left[\frac{T - T_{room}}{T_{melt} - T_{room}} \right]^m \right)$$

Johnson-Cook empirical material constitutive model is chosen as it is widely used (also in inverse identification studies as shown in the literature review) and a large number of sets of parameters is available in the literature for Ti6Al4V [19]. The cutting conditions of this study (Table 1) experimentally lead to continuous chips for the 3 uncut chip thicknesses [21]. Johnson-Cook law is therefore well suited [22]. Both formulations do not require a separation criterion to form a chip, allowing to avoid the inclusion of damage in the material behaviour description and to decrease the number of parameters to be identified. Chip formation consequently occurs through plastic deformation. The ALE formulation is moreover known to be unable to produce segmented chips with a morphology close to the experimental one [22]. The inelastic heat fraction is set to 0.9.

Table 1. Cutting conditions and materials properties [23–25]

Cutting speed, v_c (m/min)	30	
Uncut chip thickness, h (mm)	0.04, 0.06, 0.1	
Width of cut, b (mm)	1	
Cutting edge radius, r_β (μm)	20	
Rake angle, γ_0 ($^\circ$)	15	
Clearance angle, α_0 ($^\circ$)	2	
Yield stress, A (MPa)	Ti6Al4V	997.9
Young's modulus, E (GPa)	Ti6Al4V	113.8
	WC	800
Poisson's ratio, ν	Ti6Al4V	0.34
	WC	0.2
Density, ρ (kg/m^3)	Ti6Al4V	4430
	WC	15 000
Conductivity, k (W/mK)	Ti6Al4V	7.3
	WC	100
Expansion, α (K^{-1})	Ti6Al4V	8.6×10^6
	WC	5×10^6
Specific heat, c_p (J/KgK)	Ti6Al4V	580
	WC	202
Convection, U ($\text{W/m}^2\text{K}$)	50	
Radiation, ϵ	0.3	

The tool material is tungsten carbide and it is assumed to have a linear elastic behaviour. Friction at the tool-workpiece interface is modelled with Coulomb's formulation and all the friction energy is converted into heat.

2.1. ALE model

In the ALE model with Eulerian boundary conditions, material is flowing through the workpiece from the left (inflow) to the right and the chip (outflow) as shown in Figure 1 (a); the tool is fixed. The initial shape of the chip evolves to reach its final shape at the steady state. Thank to the Eulerian step in the ALE computation, elements distortion is reduced by comparison to a Lagrangian model.

ALE modelling is adapted from Kugalur Palanisamy et al. [11] to take into account limitations of the CEL implementation in Abaqus. Convection and radiation on the workpiece are removed to only include convection and radiation on the tool (see Figure 1). Gap conductance at the tool-workpiece interface is adapted from distance-based (from 0 $\text{W/m}^2\text{K}$ when the contact is open to 1×10^6 $\text{W/m}^2\text{K}$ when the contact is closed) to pressure-based (from 0 $\text{W/m}^2\text{K}$ when contact pressure is 0 MPa to 1×10^6 $\text{W/m}^2\text{K}$ when contact pressure is at least 100 MPa).

The elements size is $5 \mu\text{m} \times 5 \mu\text{m}$ close to the tool in accordance with previous studies [11]. Their size slightly increase when moving to the bottom of the workpiece to reduce computation time without influencing the results. To give an order of magnitude, the ALE model for $h = 0.1$ mm is made of 3883 CPE4RT elements (4-node linear 2D Lagrangian elements with coupled mechanical-thermal behaviour and reduced

integration) in the workpiece and 230 CPE4RT elements in the tool for a total of 4298 nodes. Mass scaling factor of 1000 is adopted as previously validated [11]. Approximately 75 minutes are needed to compute 4 ms on 4 cores of an Intel i7-5700HQ CPU at 2.7 – 3.5 GHz.

2.2. CEL model

The CEL formulation is available only in 3D in Abaqus. Boundary conditions are applied in the out-of-plane direction to be in plane strain conditions and a single element is used in that direction [26, 27]. The tool is modelled as a Lagrangian body, while the workpiece is a Eulerian body. It is therefore necessary to mesh the area where the chip will form. The Eulerian formulation of the workpiece avoids any mesh distortion. The initial configuration of the model is shown in Figure 1 (b) where the tool is fixed and the workpiece material moves from the left to the right at the cutting speed. Convection and radiation to the tool are applied, as well as pressure-based gap conductance between the tool and the workpiece, similarly to the ALE model.

The elements size is $5 \mu\text{m} \times 5 \mu\text{m}$ close to the tool according to previous mesh sensitivity investigations [26]. As for the ALE model, their size slightly increase when moving to the bottom of the workpiece to reduce computation time with no impact on the results. For $h = 0.1 \text{ mm}$, the model is composed of 4560 EC3D8RT elements (8-node linear 3D Eulerian elements with coupled mechanical-thermal behaviour and reduced integration) for the workpiece and 257 C3D8T elements (8-node linear 3D Lagrangian elements with coupled mechanical-thermal behaviour) for the tool, and a total of 10 086 nodes. Mass scaling is adopted and approximately 105 minutes are needed to compute 4 ms on 4 cores of an Intel i7-5700HQ CPU at 2.7 – 3.5 GHz.

3. Inverse identification of input parameters

The optimization problem to solve is complex: the computational cost of each point (i.e. the computation of a FE model) is high and the objective function is non-linear with potentially several local minima without a global minimum. Consequently, the parameters of both Johnson-Cook and Coulomb’s models were simultaneously inversely identified with an EGO surrogate-guided optimization for the ALE-Eulerian model and $h = 0.1 \text{ mm}$ [11]. Bayesian Optimization was adopted as it allows to select the next design point based on both the prediction of the surrogate model and its uncertainty. The budget of the optimization was 300 FE computations. The identified parameters are B, C, m, n and μ . A was not included in the identification as it is the yield stress at room temperature (Table 1).

The three quantities (i.e. the observables) available in the experimental reference [21]: the RMS value of the cutting and feed forces, F_c and F_f , respectively, and the chip thickness, h' , are used to assess the difference with the numerical model. Strain values in the workpiece, temperature values in the workpiece and the tool, chip contact length, etc. are other relevant observables to be included when available to improve the identification process. The multi-objective problem (3 observables) was transformed in a single-objective problem by using a Weighted Sum Model [11]. Two different sets of coefficients were investigated to assess their impact on the identification. The same weight was given to the observables in the first set, while the second set gave more importance to the forces (cutting followed by feed) than to the chip thickness as in industrial practice. The space in which the parameters can be found (i.e. the bounds) was obtained from the ranges of values of 20 sets of Johnson-Cook parameters available in the literature for Ti6Al4V [19], while the friction coefficient ranges from 0 to 1.

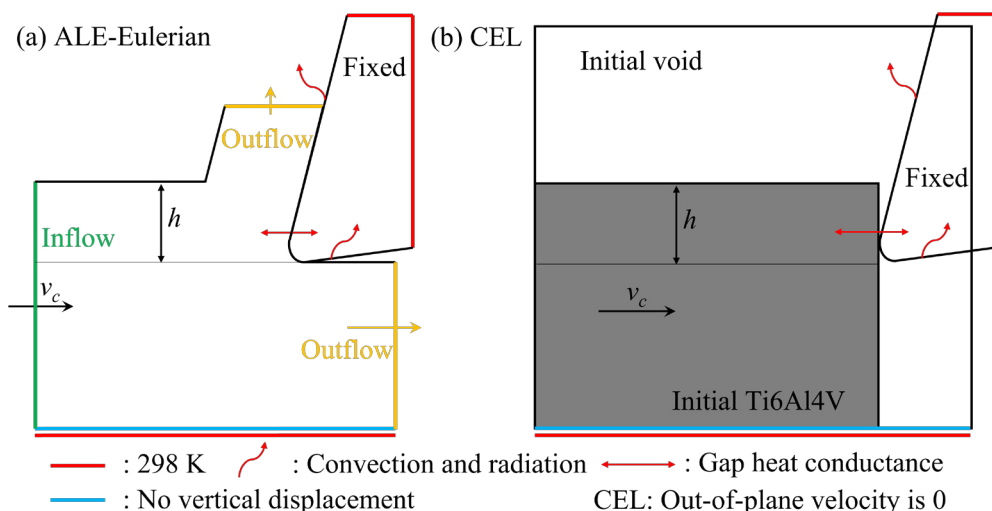


Fig. 1. Boundary conditions and initial geometries of (a) ALE-Eulerian model and (b) CEL model

4. Results and discussion

4.1. Uncut chip thickness of 0.1 mm

The 2 sets of identified parameters, M_1 and M_2 , are provided in Table 2 together with the reference set from the literature, M_0 . This reference set allows to assess the performance of the optimization. Johnson-Cook parameters from Seo et al. [23] were highlighted in a previous study [19] as the best set among 20 available for the same cutting conditions. The friction coefficient comes from Rech et al. [28] and was also used in that study. Each optimization took approximately 8 days to complete on 6 cores of an Intel i7-10700 at 2.9 – 4.8 GHz.

Table 2. Identified and reference parameters sets

Set	B (MPa)	C	m	n	μ
M_0 [23, 28]	653.1	0.0198	0.7000	0.450	0.20
M_1	331.2	0.0500	0.6440	0.594	0.19
M_2	331.2	0.0500	0.6437	0.620	0.24

Figure 2 presents an example of results for both models. The results of the 2 formulations and the 3 sets of parameters for the 3 observables are given in Figures 3 to 5 and in Table 3, and are compared with the experimental reference. It must be noted that for the ALE-Eulerian model, as shown in Figures 3 to 5, the results are slightly different than in Kugalur Palanisamy et al. [11] due to the changes introduced in the model to be in the same conditions as the CEL model. The difference between a numerical value and the experimental reference is computed as $\Delta i = \frac{|i^{(sim)} - i^{(exp)}|}{i^{(exp)}} \times 100$. The total difference between a model and the experiments is $\Delta_{Total} = \sum \Delta i = \Delta F_c + \Delta F_f + \Delta h'$, while the difference for the forces is $\Delta_{Forces} = \Delta F_c + \Delta F_f$.

For both ALE and CEL models, almost all observables are improved with the parameters from optimizations compared to M_0 . Improvements are the largest for h' followed by F_f ; F_c was already well modelled. The forces are even better modelled for M_2 than for M_1 with a difference with the experiments divided by 2 for M_2 by comparison to M_1 . As expected for M_2 , the difference with the experiments is $\Delta h' > \Delta F_f > \Delta F_c$ in accordance with the weight coefficients. The cutting force values are moreover in the experimental dispersion and F_f is close to it. On the contrary, F_c is less well modelled by M_1 than by M_0 , but

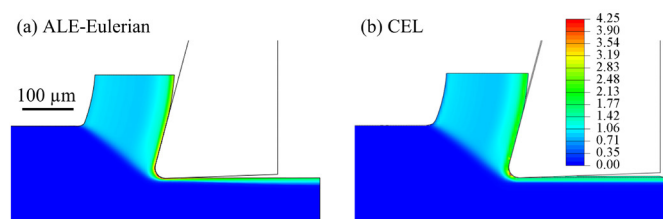


Fig. 2. Equivalent plastic strain contours at $h = 0.1$ mm with M_2 after 4 ms (a) ALE-Eulerian model and (b) CEL model

Table 3. Total and forces differences with the experimental results, Δ_{Total} and Δ_{Forces} ; best (lowest) difference values for each model at each h in **bold**

h (mm)	Δ (%)	ALE M_0	CEL M_0	ALE M_1	CEL M_1	ALE M_2	CEL M_2
0.1	Total	62	79	23	29	20	26
	Forces	21	38	12	19	6	9
0.06	Total	53	81	40	28	40	36
	Forces	13	33	26	4	20	8
0.04	Total	64	53	47	18	45	16
	Forces	23	19	42	3	33	1

the differences for M_0 are larger for F_f and h' leading to less good global (Δ_{Total}) and forces (Δ_{Forces}) performances than M_1 .

For both optimized sets, CEL better models F_c than ALE, while it is the contrary for F_f and h' . Globally, the ALE formulation provides better results (Δ_{Total} and Δ_{Forces}) than the CEL formulation. This was already true with parameters from M_0 . From these results, M_2 set of parameters is recommended for both ALE and CEL formulation.

4.2. Uncut chip thicknesses of 0.04 mm and 0.06 mm

For $h = 0.04$ mm and $h = 0.06$ mm, and both ALE and CEL models, F_c and h' are improved by comparison with M_0 . With the reference parameters M_0 , performance for F_f was quite good (with a difference of less than 10% for $h = 0.06$ mm). A degradation of the prediction (overestimation) of F_f with ALE is observed, but it is not large enough to degrade the global indicator Δ_{Total} , even if the forces indicator Δ_{Forces} is less good than M_0 . On the contrary, F_f is also improved for CEL. More generally, forces for CEL are very well modelled with differences (Δ_{Forces}) of less than 5% in 3 out of the 4 cases with optimized parameters. The chip thickness is still overestimated by both models and all sets of parameters.

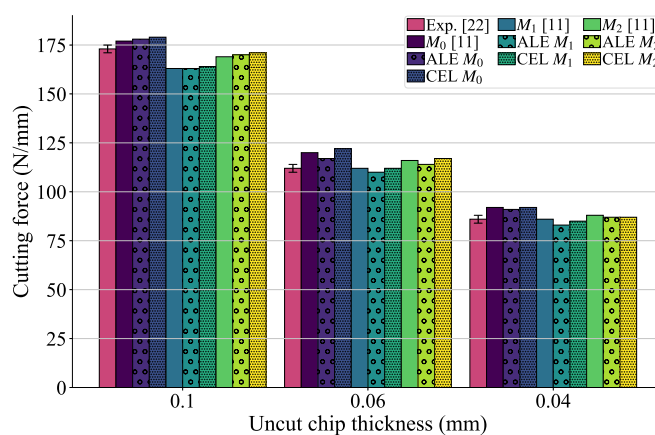


Fig. 3. Comparison of the RMS cutting force (related to the width of cut), F_c , for the 9 models with the experimental reference at the 3 different h values

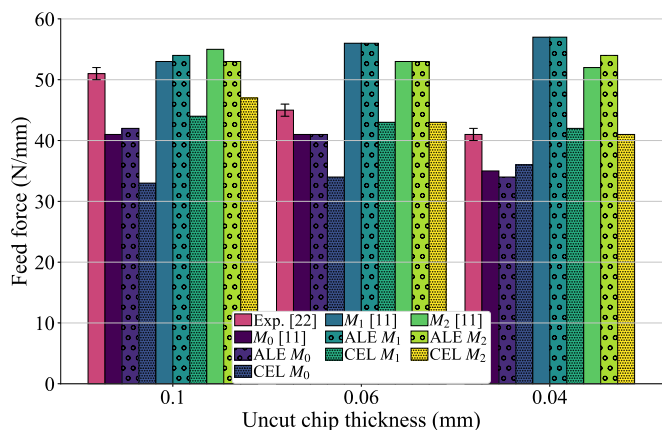


Fig. 4. Comparison of the RMS feed force (related to the width of cut), F_f , for the 9 models with the experimental reference at the 3 different h values

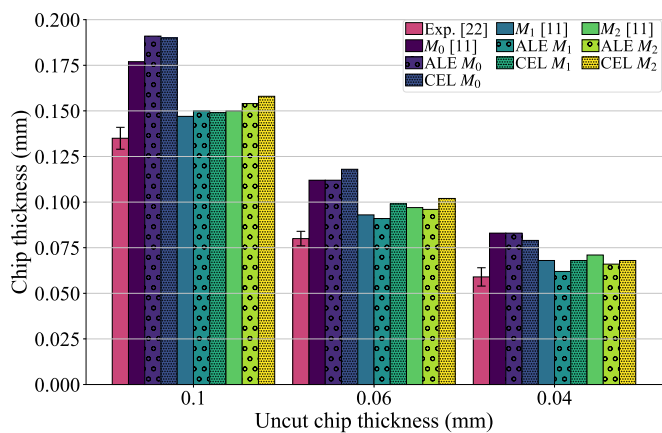


Fig. 5. Comparison of the chip thickness, h' , for the 9 models with the experimental reference at the 3 different h values

For $h = 0.06$ mm and contrary to $h = 0.1$ mm, results of M_1 are better than M_2 for CEL. For ALE, M_2 is still the recommended set and particularly for the forces. For $h = 0.04$ mm, M_2 is again the best for ALE. The M_2 set of parameters is also the best for CEL with virtually no difference with the mean experimental values of the forces.

4.3. Discussion

For all uncut chip thicknesses and sets of optimized parameters, the cutting force and the chip thickness are improved by comparison with the reference set of parameters for ALE. The feed force is however less good for $h = 0.04$ mm and $h = 0.06$ mm, values for which the identification was not performed, showing the non-uniqueness of the solution of the optimization. On the contrary, the 3 observables are improved with both sets of optimized parameters and CEL. Both total difference and forces difference decrease with the chip thickness for CEL, while they increase for ALE. This shows that the identified sets of parameters perform better for the uncut chip thickness at which they were identified for ALE, while they are better for smaller uncut chip thicknesses for CEL. That trend with the

uncut chip thickness can also be observed for CEL and forces for the reference set of parameters, not for the chip thickness. There is no clear trend for ALE and the reference set of parameters when the uncut chip thickness decreases. The update of the thermal boundary conditions of the ALE model from [11] to be the same as in the CEL model leads to changes up to 4% for the forces and up to 10% for the chip thickness. Although significant, these differences are within the experimental deviations.

The results depend on the formulation and on the uncut chip thickness. It consequently turns out to be necessary to perform the identification for several cutting conditions in the frame of a multi-objective optimization and not a single-optimization any more.

Looking at the results when the uncut chip thickness decreases, the expected trends are met for the cutting force and the chip thickness for both formulations. For ALE and the reference set of parameters, the feed force decreases with the uncut chip thickness as expected, while it does not change much with the sets of optimized parameters and has an increasing trend. On the contrary, for CEL and the reference set of parameters, the trend of the feed force was problematic as it increases when the uncut chip thickness decreases. For the sets of optimized parameters, variations with the uncut chip thickness are still small but a decreasing trend as in the experiments is observed.

Globally, the feed force is more or less constant for the 3 uncut chip thicknesses considered, except for the set of optimized parameters M_2 and CEL. This shows the complex links between the material behaviour and friction, justifying to include both of them in the identification process. The relevance of the choice of Coulomb’s friction can be questioned as it does not include the sticking region close to the cutting edge radius of the tool [2], although it takes importance when the uncut chip thickness decreases for a constant radius, and therefore impacts the chip formation mechanism. Another aspect is the fraction of the work involved in the cutting process due to friction that depends on the uncut chip thickness for constant cutting conditions as shown by Schulze et al. [29]. More appropriate friction models should therefore be considered, such as models depending on pressure, velocity and contact temperature [29], to better simulate the influence of the uncut chip thickness.

5. Conclusions and future works

This study dealt with the comparison of the ALE and CEL formulations to assess the impact of the formulation, and the parameters of the material constitutive model and the friction coefficient on the results of an orthogonal finite element model of Ti6Al4V. The sets of parameters previously identified using an EGO surrogate-guided optimization for an ALE-Eulerian model at an uncut chip thickness of 0.1 mm have been applied to a CEL model and that ALE model (updated to have the same thermal exchange conditions) at 3 uncut chip thicknesses (0.1 mm, 0.06 mm and 0.04 mm).

The results showed that the optimized parameters lead to better results for the ALE model (62% to 20% difference with

the experiments) than the CEL model (79% to 26%) at the uncut chip thickness of 0.1 mm, even if a significant improvement is noted for the CEL model. For other uncut chip thicknesses, the CEL model performed better than the ALE model (less than 5% versus more than 20% for the forces). One set of optimized parameters, M_2 , resulted globally in the closest numerical results to the experiments for both formulations.

Although the non-uniqueness of the solution was shown, the identified sets of parameters, M_2 with the CEL model for example, allowed to predict the machining forces over the whole range of feed with a performance far better than what can be achieved with some other models and input data (maximum error is of 8% for the feed force at $h = 0.1$ mm). It is moreover within the deviation commonly observed in the experiments. The performance was lower for the chip thickness, but it is more difficult to assess and with a larger deviation (the influence of the measuring procedure and method is larger than for the forces).

Future works should include several cutting conditions for the identification to move from single- to multi-objective optimization. More complex and advanced material models (e.g. including damage) and friction models were not considered at this stage. They will be included in future works to assess the improvement they might bring as the developed framework can handle them.

Acknowledgements

Financial support from Basque government project Elkartek 2022 (KK-2022/00001), and from Spanish Ministry of Sci., Innov. and Univ. project SURFNANOCUT (RTI2018_095463-B-C21/C22).

References

- [1] P. J. Arrazola, T. Özel, D. Umbrello, M. Davies, I. S. Jawahir, Recent advances in modelling of metal machining processes, *CIRP Annals* 62 (2013) 695–718.
- [2] S. N. Melkote, W. Grzesik, J. Outeiro, J. Rech, V. Schulze, H. Attia, P.-J. Arrazola, R. M'Saoubi, C. Saldana, Advances in material and friction data for modelling of metal machining, *CIRP Annals* 66 (2017) 731–754.
- [3] H. Kolsky, An Investigation of the Mechanical Properties of Materials at very High Rates of Loading, *Proc. Phys. Soc. B* 62 (1949) 676.
- [4] G. I. Taylor, The testing of materials at high rates of loading, *Journal of the Institution of Civil Engineers* 26 (1946) 486–519.
- [5] A. Shrot, M. Bäker, Determination of Johnson–Cook parameters from machining simulations, *Comput Mater Sci* 52 (2012) 298–304.
- [6] P. Bosetti, C. Maximiliano Giorgio Bort, S. Bruschi, Identification of Johnson–Cook and Tresca's Parameters for Numerical Modeling of AISI-304 Machining Processes, *J Manuf Sci Eng* 135 (2013) 051021.
- [7] B. Denkena, T. Grove, M. A. Dittrich, D. Niederwestberg, M. Lahres, Inverse Determination of Constitutive Equations and Cutting Force Modelling for Complex Tools Using Oxley's Predictive Machining Theory, *Procedia CIRP* 31 (2015) 405–410.
- [8] T. Bergs, M. Hardt, D. Schraknepper, Determination of Johnson–Cook material model parameters for AISI 1045 from orthogonal cutting tests using the Downhill-Simplex algorithm, *Procedia Manuf* 48 (2020) 541–552.
- [9] M. Hardt, D. Schraknepper, T. Bergs, Investigations on the Application of the Downhill-Simplex-Algorithm to the Inverse Determination of Material Model Parameters for FE-Machining Simulations, *Simul Model Pract Theory* 107 (2021) 102214.
- [10] M. Hardt, D. Jayaramaiah, T. Bergs, On the Application of the Particle Swarm Optimization to the Inverse Determination of Material Model Parameters for Cutting Simulations, *Modelling* 2 (2021) 129–148.
- [11] N. Kugalur Palanisamy, E. Rivière Lorphèvre, M. Gobert, G. Briffoteaux, D. Tuytens, P.-J. Arrazola, F. Ducobu, Identification of the Parameter Values of the Constitutive and Friction Models in Machining Using EGO Algorithm: Application to Ti6Al4V, *Metals* 12 (2022) 976.
- [12] J. C. Outeiro, D. Umbrello, R. M'Saoubi, I. S. Jawahir, Evaluation of Present Numerical Models for Predicting Metal Cutting Performance And Residual Stresses, *Machining Science and Technology* 19 (2015) 183–216.
- [13] P. Sridhar, J. M. Rodríguez Prieto, K. M. de Payrebrune, Discretization approaches to model orthogonal cutting with Lagrangian, Arbitrary Lagrangian Eulerian, Particle Finite Element method and Smooth Particle Hydrodynamics formulations, *Procedia CIRP* 93 (2020) 1496–1501.
- [14] M. Afrasiabi, J. Saelzer, S. Berger, I. Iovkov, H. Klippel, M. Röthlin, A. Zabel, D. Biermann, K. Wegener, A Numerical-Experimental Study on Orthogonal Cutting of AISI 1045 Steel and Ti6Al4V Alloy: SPH and FEM Modeling with Newly Identified Friction Coefficients, *Metals* 11 (2021) 1683.
- [15] F. Ducobu, E. Rivière-Lorphèvre, E. Filippi, Application of the Coupled Eulerian-Lagrangian (CEL) method to the modeling of orthogonal cutting, *Eur J Mech A Solids* 59 (2016) 58–66.
- [16] F. Ducobu, P.-J. Arrazola, E. Rivière-Lorphèvre, G. Zarate, A. Madariaga, E. Filippi, The CEL Method as an Alternative to the Current Modelling Approaches for Ti6Al4V Orthogonal Cutting Simulation, in: *Procedia CIRP*, volume 58, 245–250 (2017).
- [17] A. Aridhi, T. Perard, F. Valiorgue, C. Courbon, J. Rech, A. Brosse, M. Girnon, B. Truffart, H. Karaoui, Comparison of the CEL and ALE approaches for the simulation of orthogonal cutting of 15-5PH and 42CrMo4 materials, *Proceedings of the Institution of Mechanical Engineers, Part B: Journal of Engineering Manufacture* (2022) 09544054221136390.
- [18] Y. Zhang, J. C. Outeiro, T. Mabrouki, On the Selection of Johnson-cook Constitutive Model Parameters for Ti-6Al-4V Using Three Types of Numerical Models of Orthogonal Cutting, *Procedia CIRP* 31 (2015) 112–117.
- [19] F. Ducobu, E. Rivière-Lorphèvre, E. Filippi, On the importance of the choice of the parameters of the Johnson–Cook constitutive model and their influence on the results of a Ti6Al4V orthogonal cutting model, *Int J Mech Sci* 122 (2017) 143–155.
- [20] G. Johnson, W. Cook, A constitutive model and data for metals subjected to large strains, high strain rates and high temperatures, in: *Proc. 7th International Symposium on Ballistics*, volume 21, The Hague, The Netherlands, 541–547 (1983).
- [21] F. Ducobu, E. Rivière-Lorphèvre, E. Filippi, Experimental contribution to the study of the Ti6Al4V chip formation in orthogonal cutting on a milling machine, *Int J Mater Form* 8 (2015) 455–468.
- [22] F. Ducobu, E. Rivière-Lorphèvre, E. Filippi, Numerical contribution to the comprehension of saw-toothed Ti6Al4V chip formation in orthogonal cutting, *International Journal of Mechanical Sciences* 81 (2014) 77–87.
- [23] S. Seo, O. Min, H. Yang, Constitutive equation for Ti–6Al–4V at high temperatures measured using the SHPB technique, *Int J Impact Eng* 31 (2005) 735–754.
- [24] GRANTA EduPack 2020, Granta Design Limited, 2020.
- [25] M. Boivineau, C. Cagran, D. Doytier, V. Eyraud, M. H. Nadal, B. Wilthan, G. Pottlacher, Thermophysical Properties of Solid and Liquid Ti-6Al-4V (TA6V) Alloy, *Int J Thermophys* 27 (2006) 507–529.
- [26] F. Ducobu, E. Rivière-Lorphèvre, E. Filippi, Mesh influence in orthogonal cutting modelling with the Coupled Eulerian-Lagrangian (CEL) method, *Eur J Mech A Solids* 65 (2017) 324–335.
- [27] F. A. V. da Silva, J. C. Outeiro, Machining simulation of Inconel 718 using Lagrangian and Coupled Eulerian-Lagrangian approaches, *Procedia CIRP* 102 (2021) 453–458.
- [28] J. Rech, P. J. Arrazola, C. Claudin, C. Courbon, F. Pusavec, J. Kopac, Characterisation of friction and heat partition coefficients at the tool-work material interface in cutting, *CIRP Annals* 62 (2013) 79–82.
- [29] V. Schulze, F. Bleicher, C. Courbon, M. Gerstenmeyer, L. Meier, J. Philipp, J. Rech, J. Schneider, E. Segebade et al., Determination of constitutive friction laws appropriate for simulation of cutting processes, *CIRP Journal of Manufacturing Science and Technology* 38 (2022) 139–158.